Open Access

Iraqi Journal of Industrial Research (IJOIR)

Journal homepage: http://ijoir.gov.iq

Enhancing Anticorrosive Characteristics of Epoxy through Nanocellulose Reinforcement

Rafah Alwan Nassif*, Raghad Hamid Hilal, Wafaa Khalid Khalef

Department of Applied Science, University of Technology, Iraq

Abstract

Nanocellulose (NC) stands out as a promising reinforcement agent for protective coatings due to its renewable, biodegradable, and biocompatible nature. In this research, we synthesized coconut shell powder nanoparticles (CSNPs) with an average size of 52.43 nm in the laboratory. These CSNPs were incorporated into epoxy (EP) coatings at loadings ranging from 0 to 3 wt% through a hand-laying process, applied onto steel rods at room temperature. Characterization techniques such as X-ray diffraction (XRD) and scanning electron microscopy (SEM) were employed to analyze the nanocomposite coatings. The corrosion resistance of the coated steel rods was evaluated using electrochemical impedance spectroscopy (EIS) after immersion in a 3.5% sodium chloride solution. Notably, after a 5-day exposure, the 2% CSNP-loaded coating exhibited the highest adhesion strength, surpassing the pure epoxy coating and other formulations. SEM analysis confirmed the excellent dispersion of 2% nanocellulose in the matrix, demonstrating superior anti-corrosion properties over 30 and 90 days of EIS experiments. Comparative studies with pure epoxy resin through EIS and potentiodynamic polarization (PDP) tests underscored the significant enhancement in corrosion protection performance achieved by incorporating CSNPs. The study employs terms such as nanocomposites, nanocellulose, characterizations, coating, anticorrosion, and electrochemical tests to comprehensively address the multifaceted aspects of this investigation.

1. Introduction

Materials, especially metals, degrade naturally through corrosion. Chemical or electrochemical interactions between a material and its surroundings cause it [1]. Corrosion harms industries, ecosystems, and infrastructure and costs the economy significant money. Corrosion has huge economic repercussions. Corrosion costs trillions worldwide [2]. By blocking corrosive processes, corrosion protection coatings stop or delay them [3]. These coatings protect the material from moisture, oxygen, chemicals, and contaminants [4]. Many industries need corrosion-resistant coatings. Preventing corrosion damage to materials, infrastructure, and ecosystems requires corrosion protective coatings [1-4]. Polymer nanocomposite refers to a composite material consisting of reinforced fillers, wherein at least one dimension of the filler is less than 100 nm in size. A nanocomposite is a brand-new type of nanostructured hybrid material that stands out due to the inclusion of infill material with

nanostructural characteristics. [5]. the bio nanocomposite component may consist of inorganic or organic, organic or inorganic, or inorganic or organic sources; therefore, it can be classified into two categories: nanofiller material reinforced with petroleum-derived polymers (e.g., epoxies, polypropylene (PP), and polyester (PE); or nanofiller material composed of inorganic or synthetic nanofillers (e.g., ZnO nanoparticulate, nanofiber cellulose (NFCs), or bacterial nanocellulose (BNCs)). Nanocellulose composites find utility in a variety of contexts, including but not limited to the production of lithium-ion batteries, fuel cells, solar cells, loudspeaker membranes, packaging, foldable substrates for electronic devices, biomedical battery membranes, and battery membranes [7]. Epoxy and other thermoset polymers are frequently found in adhesives, paints, and surface coatings. Similar to other thermosetting materials, epoxy resins are exceedingly brittle, which restricts their application to products requiring high impact and fracturing strength. Recent studies have suggested that certain nanoparticles, such as NFC, have the potential to improve the mechanical properties of coatings coated with epoxy [8, 9].

As a result, several studies have focused on modifying the phase stability of polymer blends using nanoparticles. W. Hou and colleagues compared the anticorrosion performance of epoxy coatings containing two types of nano polyaniline on Q235 steel and discovered that epoxy coatings containing PANI obtained in the FeCl2/H2O2 system had the best corrosion protection performance of the three systems studied, and they discussed the possible protective mechanisms of PANI [10]. Poaty et al. modified cellulose nanocrystals with various acryloyl chlorides as reinforcing derivatives from wood coatings, resulting in increased abrasion resistance of the coatings [11]. Sh. Ammar and his colleagues looked at how water and solvent as carrier agents affected the overall characteristics of epoxy resin. In addition, four concentrations of copper pigments (Cu) were effectively incorporated in two polymeric matrixes, and the changes in fouling ability, structural, thermal, morphological, and anticorrosion performance were investigated. [12]. Iling A. et al. created a number of coatings using epoxy and varying amounts of nanocellulose and applied them to mild steel under normal conditions. The 1% nanocellulose composite coating system showed the best anti-corrosion capabilities, which were verified by 30-day EIS research [13]. CleideBorsoi and his colleagues investigated the corrosion prevention of mild steel using cellulose, polyaniline-emeraldine-salt (PAni ES), and amino propyl triethoxy silane (APTES) epoxy coatings. Even after 90 days of immersion in a 3.5 wt% NaCl solution, polymer coatings containing carbon nano walls (CNW) and PAni demonstrated excellent corrosion protection. The corrosion resistance of epoxy coating with additional CNW functionalized with PAni improved the most, demonstrating a positive interaction between a conducting polymer's electroactivity and nanoscale cellulose particles [14]. Graphene-epoxy composites for anti-corrosion coatings on steel substrates were investigated by Benhalima A. et al. They discovered that greater graphene nanoparticles (GNP) concentrations above 1% lead to an improvement in anti-corrosion performance [15].

Coconut shell-derived cellulose nanoparticles were prepared in the laboratory at concentration ranging from 1 to 3 wt%. These nanoparticles were employed to manufacture NC/epoxy composite coatings in this investigation. The morphology of the produced nanocomposites was studied using a scanning electron microscope (SEM). Electrochemical impedance spectroscopy (EIS) was used to evaluate the protective qualities of pure and nanocomposite coatings. Furthermore, the adhesion strength and thickness of the resulting coatings were tested.

2. Experimental Procedure
2.1. Materials
Epoxy resin (Sikadur-105) with a density of 1.04g/cm3and it's hardened in a ratio of 4:1were used. Coconut shell was collected from Iraqi markets and sodium chloride was purchased from the chemical labrortory.

2.2. Preparation of Coconut Shell Nanoparticles (CSNPs)
The coconut shells were dried in the sun for several days before being crushed into small pieces with a hammer, then ground into powder with varying granular sizes and sieved using sieves ranging in size from 650 to 63 m. A high-energy ball mill was utilised for 70 hours at a speed of 180 rpm at a rate of 7 hours per day to obtain nanoparticles. The balls are composed of stainless steel and range in diameter from 19mm to 12mm. Finally, the nanoparticles were dried in an oven at 80 °C for an hour before being cooled in desiccators. The coconut shell nanoparticles CSNPs were subsequently analyzed using an X-ray fluorescence spectrometer and a scanning electron microscope.

2.3. Preparation of Nanocomposites

Various amounts of CSNPs were added to epoxy resin in weight ratios of 1, 2, and 3 wt%. The mixture was mechanically agitated for minutes with a glass rod and then sonicated for 30 seconds for dispersion. The hardener was then added to the mixture at a 4:1 ratio. Brushing the mixture onto mild steel was used. The coated mild steel was cured at ambient temperature for several days to achieve a consistent protective coating for the anticorrosion test. The thickness of the dry coating was calculated to be 75± 13 mm.

2.4. Characterization

The pull-off technique was used for measuring the coating adhesion in accordance with ASTM D4541-2009 using PosiTest Pull-Off Adhesion Tester from DeFelsko Corporation in Ogdensburg, New York, US. The values for the pull-off strength loss were computed using equation (1).

$$The\ pull-off\ strength = \frac{a-b}{a} \times 100\% \ \dots\dots(1)$$

Where a and b represent the wet pull-off strength and dry pull-off strength, respectively, after 7 days of immersion in a 3.50% NaCl solution. Every measurement was made three times.

The coating's thickness was measured using a Sndway SW-6310C coating thickness meter (Shenzhen, Guangdong, China).

SEM (DSM 962, Zeiss) was used to analyze the sample's morphology. The Miniflex XRD system from Japan's Rigaku was used for obtaining XRD patterns of ZnO NPs.

To evaluate corrosion resistance regarding different coatings in 3.5% NaCl solution, use a CHl660D electro-chemical analyzer and test methods for electrochemical corrosion. Potentiodynamic polarization and EIS have been recorded for the coated and uncoated iron coupons with the use of a 3-electrode electro-chemical cell with the saturated calomel electrode (SCE) as reference electrode, platinum gauze as the counter electrode, and the iron coupons as working electrode. EIS was after that used to assess the epoxy coatings' ability to protect steel surfaces from corrosion. The experiment was carried out using an AUTOLAB 86183 with amplitude and frequency ranges of 10 mV and 100 kHz-0.01 Hz, respectively. Electro-chemical parameters, like the corrosion current (Icorr), corrosion potential (Ecorr), corrosion rate (CR), Tafel slopes (ba, bc), and inhibition effectiveness (IEPDP) have been determined once the measurement was done. The slope could be determined by merely measuring slope of every one of the linear segments of the curve, while the corrosion potential could be computed from the area with the lowest current density on Tafel plot. The equations below could be used to calculate the corrosion rate and inhibition efficiency given the corrosion current [25]:

$$C_R = k\frac{I_{corr}}{d}EW \ \dots\dots(2)$$

Where k represents a unit conversion factor (0.13), d represent the mild steel density (7.86g/cm3), EW represent equivalent weight (27.93g).

$$IE_{PDP} = \frac{i_{corr} - i_{corr}^{inh}}{i_{corr}} \times 100 \ \dots\dots(3)$$

Where i_{corr}^{inh} represent the corrosion current density regarding the inhibited system.

3. Results and Discussion

The XRD pattern of CSNPs is depicted in Figure (1). The x-ray diffraction pattern of CSPNs samples revealed three highest peak intensities at diffraction angles 20 and 21degree, with the low intensity peaks attributed to other elements present in the CSNPs. Based on the width of the dominating peaks indicated above, the average size of CSNPs has been found to be 52.43nm using the Debye-Scherrer equation.
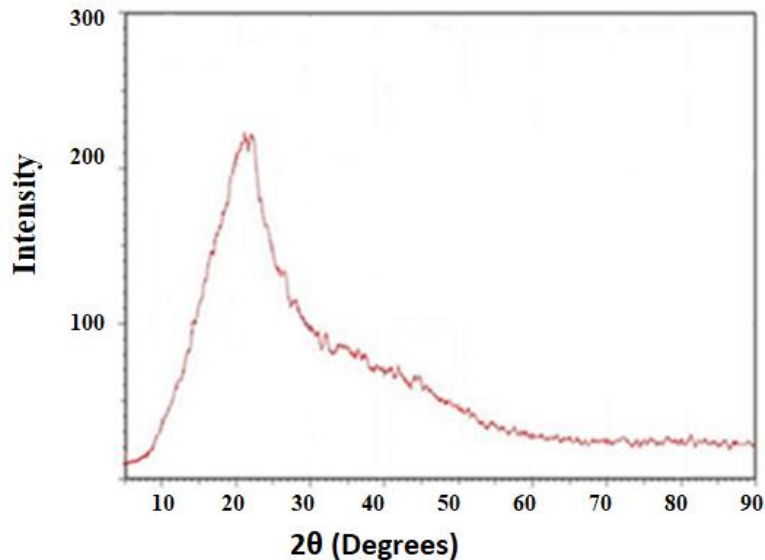
Figure (1): XRD pattern for CSNPs.

3.1. SEM of CSNPs

In a SEM image shown in Figure (2), CSNPs appeared angular, uneven, and squashed. Raw CSNPs, on the other hand, were extremely porous and had appropriately high solid densities [20]. Ball milling broke down the spherical structure of coconut shell, and particle size fell to the nanoscale with time [14]. Because of their structure, CSNPs are excellent filler components in composites [21]. A bigger, irregularly shaped carbon particle can be spotted beside the solid spheres. Interparticle fusion can also result in the formation of agglomerated spheres and irregularly shaped amorphous particles. SEM testing, even at higher magnifications, made it impossible to differentiate a single particle, which could be attributed to particle aggregation.
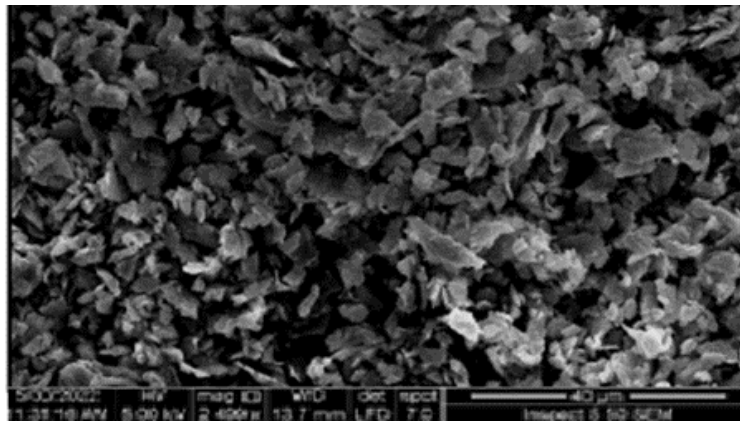
Figure (2): SEM of coconut nanoparticles at a magnification of X2499.

3.2. SEM of Coatings

As demonstrated in Figure (3a), pure epoxy has no surface characteristics; hence, it detects a smoother surface than other composites, which were found to be somewhat rough. The reason for this roughness could be that the nanoparticles in the epoxy resin generated a cross-linking process that caused the surface of the matrix to become more abrasive via dispersion, and this change in abrasiveness caused the surface of the coatings to appear rougher [22]. As a result, CSNPs reduced the smoothness of the coatings. Figure (3c) depicts the surface morphology of a 2% nanocomposite covering. It was discovered in this percentage to be relatively rough and smooth in the same neighboring location. This observation indicated that the strong intermolecular interaction inside the cross-linking pores improved the adhesion behavior of the coatings due to the stiffness of the surface [23]. While the aggregation of CSNPs in 1% and 3% was due to a heterogeneous response between CSNPs and epoxy matrix.
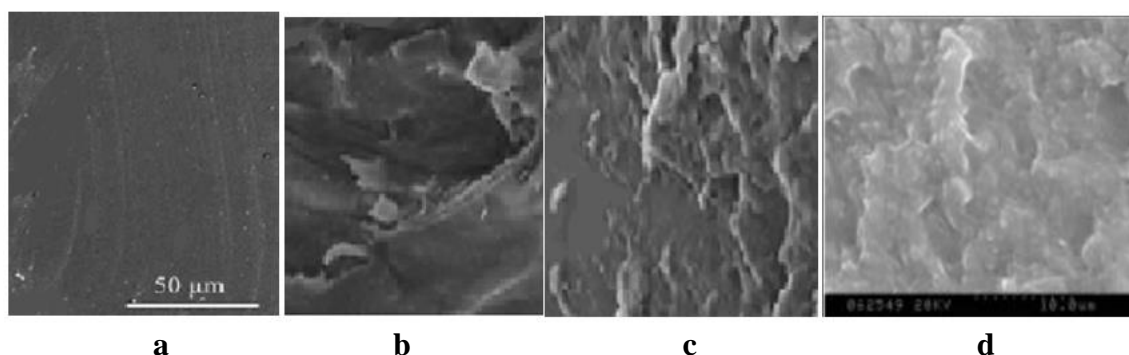
Figure (3): SEM images of (a) the neat epoxy coating magnification of X250, (b) 1%coating at a magnification of X2000, (c) 2% coating at a magnification of X250 (a) and (d) 3% coating at a magnification of X3808.

3.3. Adhesion Strength

Adhesion is the force required to remove the coating from the steel rod. Adherence is critical for a coating to have a long service life [18]. Figure (4) depicts adhesion findings for all coatings after a 7-day immersion in a 3.5% NaCl solution. The adhesion strength of the 2% coating was 12.33 MPa, compared to 7.87 and 10.45 MP for the 1% and 3% coatings, respectively. This could be due to the matrix's greater dispersion and improved compatibility with CSNPs. Pure epoxy was discovered to have a lower adhesive strength value than any other coating. Failures in both the adhesive and cohesive processes resulted in the separation of the coatings from the surface of the steel rod [15]. Cohesive failure occurs when the link of the coating to the steel surface is sufficiently strong to allow the force being applied to overcome the coating's cohesive properties. Adhesion failure occurs when the interfacial adhesion bonds are not as strong as they should be [19].
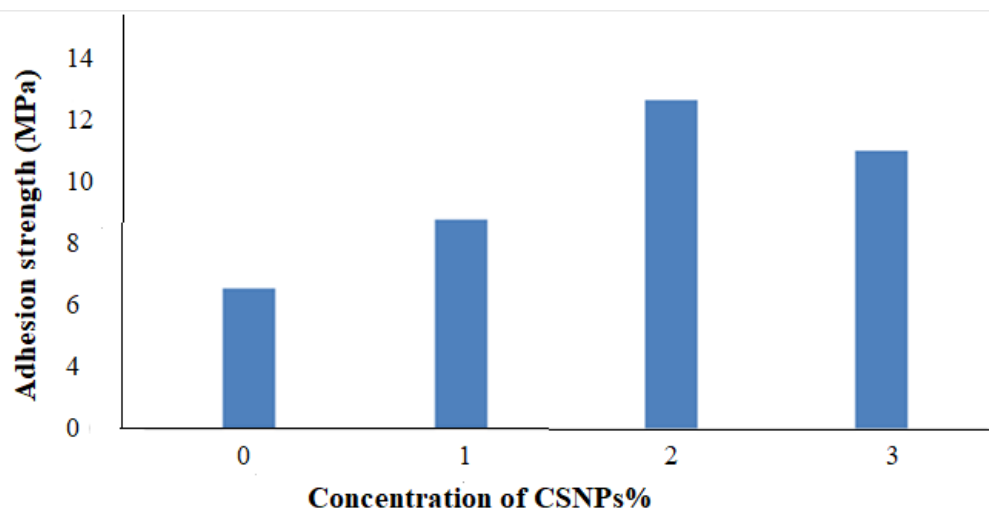
Figure (4): Adhesion strength of all samples.

4. Electrochemical Tests

4.1. Electro-chemical Impedance Spectroscopy (EIS) Measurements

The results obtained after 30 and 90 immersion days in a 3.50% NaCl solution have been graphically illustrated using EIS to evaluate the effect of CSNPs on the corrosion protection performance regarding EP, as shown in Figures (5 & 6). The impedance plot of the pure epoxy coating exhibited the lowest impedance modulus /Z/, as seen in these two figures. In contrast, after 30 and 90 days of immersion, all of the other reinforced coatings with varying concentrations of CSNPs displayed good corrosion protection properties. The reason behind the behavior of the pure epoxy coating at the tow period time is that this coating suffered permeation of electrolytes toward the surface of the substrate and weakest barrier ability [20]. In other words, the pure epoxy coating did not withstand the attacker's corrosive substance. As a result of the formation of diffusion routes and the preparation of corrosive chemicals on the substrate surface, corrosion occurs [21]. In contrast, 1% and 2%

nanocoatings appear to have better EIS performance after 30 and 90 days when compared to pure epoxy coating. The reason for this behaviour is the ability of the CNPs to block the porosity that forms in the coatings and improve the coating quality by increasing the possibility of achieving the best defect-free coating film [26]. This increased the distance travelled by corrosive chemicals to reach the substrate surface [27].
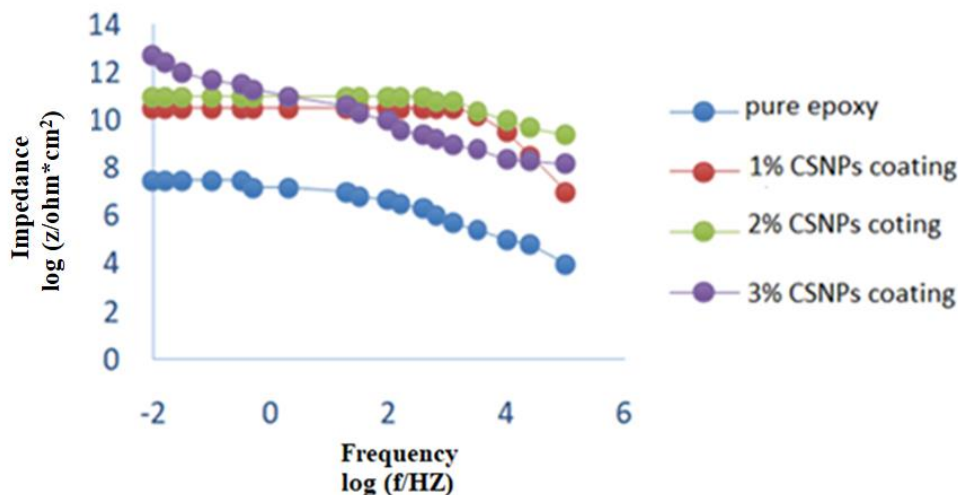

Figure (5): EIS bode plot of all coatings after 30 days of immersion.
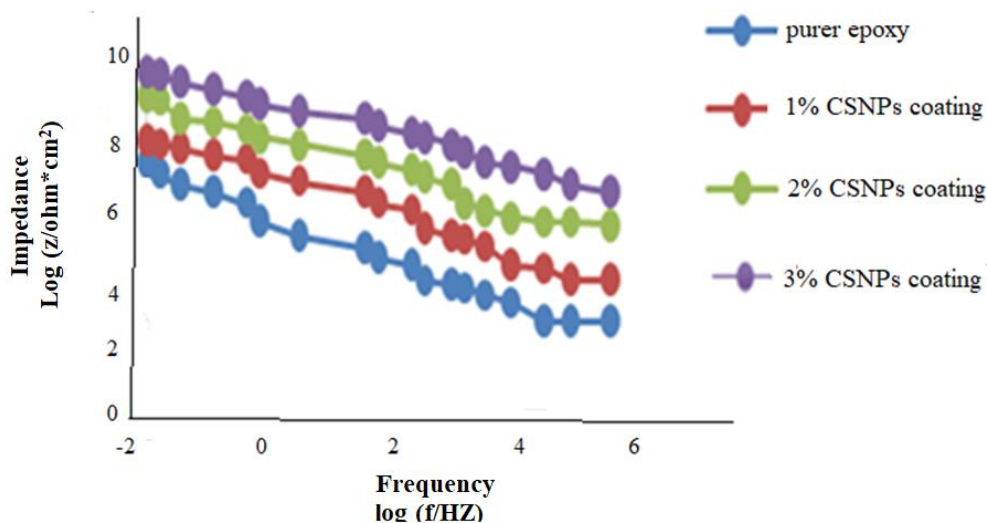

Figure (6): EIS bode plot of all coatings after 90 days of immersion.

Figure (7) depicts an analogous circuit with an electrode coated in a porous layer with two interfaces—coating/electrolyte and coating/metal. Table (1) also includes the impedance values for all resistance components associated with the used equivalent circuit model (1), where Cc is the constant phase element related to coating resistance, X is the constant phase element double layer capacitance, Z is the diffusion capacitance, Re is the electrolyte resistance, Rc is the coating resistance at high frequencies, Rct is charge transfer resistance, and R_{diff} is diffusion resistance.

Table (1): Parameters of coating/substrate systems following 90 days of immersion in 3.5wt% NaCl solution.

| Samples	$Rc(\Omega cm^2)$	$Rct(\Omega cm^2)$	$R_{diff.} (\Omega cm^2)$
Pure epoxy	$(5.22\pm0.23) \times 10^4$	$(9.52\pm0.33) \times 10^5$	$(6.33\pm0.63) \times 10^5$
1%	$(3.28\pm0.15) \times 10^8$	$(1.62\pm0.06) \times 10^9$	$(4.21\pm0.52) \times 10^5$
2%	$(2.36\pm0.87) \times 10^7$	$(6.27\pm0.22) \times 10^8$	$(7.42\pm0.47) \times 10^7$
3%	$(7.23\pm0.76) \times 10^5$	$(4.75\pm0.25) \times 10^7$	$(2.66\pm0.13) \times 10^8$
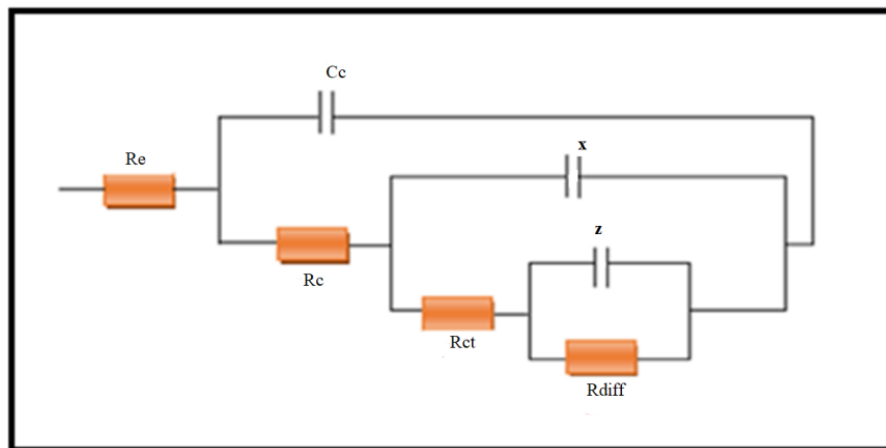
Figure (7): Equivalent electrical circuit to fit results that have been acquired following 90 days of immersion in 3.5wt% NaCl solution.

4.2. Potentiodynamic Polarization

Potentiodynamic polarization (PDP) was used to examine the electrochemical kinetics regarding coated mild steel corrosion. A crucial factor in determining corrosion damage in a system and effectiveness of protective coatings is corrosion potential. The corrosion potential related to the mild steel specimen has been found to be 450mV, which is within a range between 450mV and 465mV reported in other investigations with similar experimental setups [28-30]. According to Figure (8) and Table (2), the Ecorr value of the 3% composite coating is higher than that of the other samples, and the Ecorr increase over the steel rod was around 35%, compared to a somewhat lower value for the other samples. The mild steel had the highest Icorr and Vcorr values, which began to fall as the CSNP concentration increased. By extrapolating the Tafel plot, which is proportional to the rate of electrochemical reaction, the corrosion current density can be easily calculated experimentally. When CSNPs are used, a lower corrosion current density is better since it indicates a lower corrosion rate. The results reveal that the inhibitor molecules were adsorbed on the surface of the mild steel and delayed the electrochemical processes, as evidenced by a reduction in corrosion rate and current density [31]. Arabinose, xylose, and glucose are examples of adsorbable inhibitor chemicals found in hemicellulose. Although additional molecules may be present in CSNPs that are deposited on the surface, their impact on inhibition is negligible due to their low concentration. The performance of the inhibitor, as measured by lowering the current density, is comparable to the efficiency of inhibition. The results showed that when CSNP concentrations grew, so did the inhibition efficiency. Because more inhibitor molecules are adsorbed at higher concentrations, this results in greater surface coverage and improved inhibitory effectiveness [10]. The Table (2) also shows how the values increase abruptly and dramatically when the filler concentration increases. In general, higher PEF and Ecorr and lower CR and Icorr suggest superior corrosion resistance.

Table (2): Potentiodynamic polarization parameter values for the prepared samples after 90 day immersion.

Samples	E_{corr} (mVvs.SCE)	I_{corr} (A/cm^2)*10^{-5}	B_a (V/dec)	B_c (V/dec)	C_R (mm/year)	IE_{PDP} %
Bar steel	-450	7.43	0.621	0.121	3.432	---
Pure epoxy	-382	6.054	0.548	0.725	2.794	18.51
1%	-352	5.572	0.413	0.942	2.573	25.00
2%	-323	4.731	0.457	1.123	2.185	36.3
3%	-292	4.12	0.482	0.841	1.903	44.5
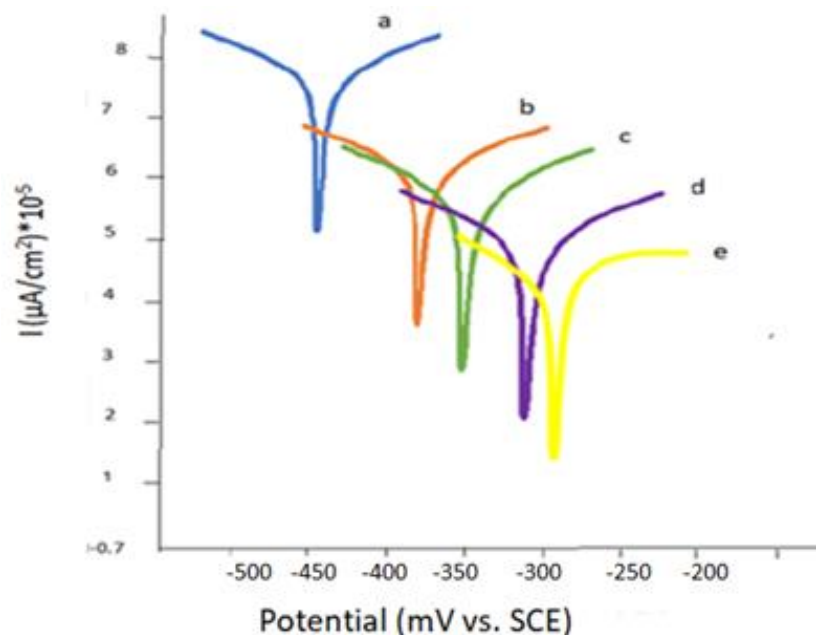
Figure (8): The potentiodynamic polarization curves of (a) uncoated rod steel, (b) the pure epoxy coating, (c) 1%CSNPs coating, (d) 2% CSNPs coatingand, and (e) 3% CSNPs coating at.

5. Conclusions

EIS studies were carried out with immersion in solution of 3.5% NaCl for 30 and 90 days to explore the barrier features and corrosion protection performance of all coatings. Nanocellulose acts as good agent for superior anti-corrosion properties in comparison with pure epoxy. So, 2% nanocellulose coating had the best barrier properties. Therefore, it considers as the better concentration to enhance the corrosion properties performance. Furthermore, PDP measurements revealed that CSNPs inhibited mild steel corrosion via a combined process of anodic and cathodic reaction retardation. As the dosage was raised, the corrosion rate and current density decreased, indicating that more inhibitor molecules have been adsorbed. The improved corrosion protection effectiveness of coatings composite is due to creation of a more uniformly passive film on steel surface, and the addition of CSNPs particles increases the tortuosity of the corrosive substance diffusion pathway.

Conflict of Interest: The authors declare that there are no conflicts of interest associated with this research project. We have no financial or personal relationships that could potentially bias our work or influence the interpretation of the results.

References

[1] B. El Ibrahimi, J. V. Nardeli and L. Guo, "An Overview of Corrosion, Sustainable Corrosion Inhibitors I: Fundamentals, Methodologies, and Industrial Applications", *ACS Sym. Ser.*, vol. 1403, pp. 1–19, 2021.

[2] H. S. Aljibori, A. Alamiery, and A. A. H. Kadhum, "Advances in corrosion protection coatings: A comprehensive review", *Int. J. Corros. Scale Inhib.*, vol. 12, no. 4, pp. 1476–1520, 2023.

[3] K. Tamalmani and H. Husin, Review on Corrosion Inhibitors for Oil and Gas Corrosion Issues, *Appl. Sci.,* vol. 10, no. 10, pp. 3389, 2020.

[4] A. Nasser, P. Ndalila, A. Mawugbe, et al., "Mitigation of Risks Associated with Gas Pipeline Failure by Using Quantitative Risk", Management Approach: A Descriptive Study on Gas Industry, *J. Mar. Sci. Eng.*, vol. 9, no. 10, pp. 1098, 2021.

[5] S. Kimiyasu, T. Uichi, A. UsukeI, et al., "Nanocelluloses and Related Materials Applicable in Thermal Management of Electronic Devices: A Review", *Nanomaterials,* vol. 10, no. 2, pp. 448-454, 2020.

[6] M. Hon, T. Lee, T. Soo, "A review of nanocellulose polymer composite characteristic and challenge", *Polymer -plastic technology and engineering*; vol. 56, no. 2, pp. 687-731, 2017.

[7] J. Mohammed, B. Sami, and H. Abdulkhalil, "Celluloce reinforced nanofiber composite", *Elsevier Ltd*.2017.

[8] P. Mingzhu, Z. Xiaoyan, and C. Minzhi "Cellulose nanowhiskers isolation and properties from acid hydrolysis combined with high pressure homogenization*", Bioresources*, vol. 8, no. 3, pp. 933-934, 2013.

[9] H. Brenda, U. Esteban, P. Sanjiv, et al., "Investigation of cellulose nanocrystals (CNC) and cellulose nanofibers (CNF) as thermal barrier and strengthening agents in pigment-based paper coatings", *Journal of Coatings Technology and Research*, vol. 19, no. 4, pp. 337–346, 2022.

[10] W. Hou, Y. Liu, and W. Zhao "Comparison study on anticorrosion performances of the epoxy coatings with two different nano-polyaniline for Q235 steel", *Materials and corrosion*, vol. 64, no. 2, pp. 960-968, 2013.

[11] P. Bouddah, V. Vahe, W. Luana, et al., "Modification of cellulose nanocrystals as reinforcement derivatives for wood coatings", *Pro.Org. Coa.t*, vol. 77, no. 77, pp. 813-820, 2014.

[12] S. Ammar, K. Ramesh, et al., "Comparison studies on the anticorrosion and overall performance of solvent/water based poxy-copper reinforced composite coatings", *Matreials Express*, vol. 6, pp. 403-413, 2016.

[13] A. Iling, S. Ammar, K. Ramesh,etal. "Anticorrosion properties of epoxy \ nanocellulose nanocomposite coating", *BioResources*, vol. 12, no. 2, pp. 2912-2929, 2017.

[14] B. Cleide, C. Lisete, J. Ademir, and A. Carlos, "Effect of the Incorporation of Micro and Nanocellulose Particles on the Anticorrosive Properties of Epoxy Coatings Applied on Carbon Steel*", Materials Research*, vol. 21, no. 3, pp. 1-10, 2018.

[15] A. Benhalima, A. Bergren, K. Bosnick, et al., "Graphene- epoxy composites for anticorrosion coatings", *Tech Connect Briefs*, vol. 1, pp. 240-243, 2018.

[16] M. Rosa, E. Medeiros, J. Malmonge, et al., "Cellulose nanowhiskers from coconut husk fibers: Effect of preparation conditions on their thermal and morphological behavior", *Carbohydrate Polymers*, vol. 8, pp. 83–92, 2010.

[17] B. Lekhasree, E. Muthusankar, and S. Vignesh, "ZNO/Cellulose Nano whiskers Reinforced Pectin for Antimicrobial Food Packaging", *International Journal of Applied Science Research (IJASR),* vol. 2, pp. 11-18, 2021.

[18] Y. Ziat, M. Hammi, Z. Zarhri, and C. Laghlimi, "Epoxy coating modified with graphene: A promising composite against corrosion behavior of copper surface in marine media", *J. Alloys Comp.*, vol. 11, pp. 820-829, 2020.

[19] R. Randy, H. Feng, H. Qian, et al., "Comparative Study of Corrosion Properties of Different Graphene Nanoplate/Epoxy Composite Coatings for Enhanced Surface Barrier Protection", *Coatings,* vol. 11, no. 3, pp. 285, 2021.

[20] D. Zaarei, A. Sarabi, F. Sharif, et al., "Preparation and Evaluation of Epoxy-Clay Nanocomposite Coatings for Corrosion Protection", *Int. J. Nano sci. and technol.*, vol. 6, no. 2, pp. 126-136, 2010.

[21] I. Wonnie, S. Ammar, K. Rameshkais, "Anticorrosion Properties of Epoxy-Nanochitosan Nanocomposite Coating", *Progress in organic coating*, vol. 113, pp. 74-81, 2017.

[22] X. Shi, T. Nguyen, et al., "Effect of nanoparticles on the anticorrosion and mechanical properties of epoxy coating", *Surface and Coatings Technology*, vol. 204, no. 3, pp. 237-245, 2009.

[23] M. Kadhum, et al., "Mechanical properties of epoxy/AL2O3 nanocomposites", *Int. J.APP. Annov. Eng. Manag.,* vol. 2, no. 11, pp. 10-16, 2013.

[24] Y. He, B. Yaman, P. Jinshan, et al., "Comparative study of CNC and CNF as additives in waterborne acrylate-based anti-corrosion coatings", *Journal of Dispersion Science and Technology*, vol. 41, pp. 2037-2047, 2020.

[25] Y. He, Y. Boluk, J. Pan, et al., "Corrosion Protective Properties of Cellulose Nanocrystals Reinforced Waterborne Acrylate-Based Composite Coating", *Corros. Sci.*, vol. 155, pp. 186–194, 2019.

[26] H. Jiwei, H. Chuanbo, and Q. Yongquan, "Preparation and Corrosion Resistance of poly(o-toluidine)/nano SiC/epoxy Composite Coating", *Int. J. Electrochem. Sci.*, vol. 10, pp. 10607-10618, 2015.

[27] B. Aghiles and D. Rachida, "Synthesis and characterization of hybrid materials based on graphene oxide and silica nanoparticles and their effect on the corrosion protection properties of epoxy resin coatings", *Journal of Adhesion Science and Technology.*, vol. 33, no. 8, pp. 834–860, 2019.

[28] H. Ferdosi and H. Tavakoli, "Electrochemical properties of a new green corrosion inhibitor derived from prosopis farcta for St37 steel in 1 M hydrochloric acid", *Met. Mater. Int.*, vol. 26, pp. 1654-1663, 2020.

[29] H. Nwankwo, E. Akpan, L. Olasunkanmi, et al., "Substituted carbazoles as corrosion inhibitors in microbiologically influenced and acidic corrosion of mild steel: Gravimetric, electrochemical, surface and computational studies", *J. Mol. Struct.*, vol. 1223, pp. 129328, 2021.

[30] A. El Aatiaoui A., M. Koudad, T. Chelfi, et al., "Experimental and theoretical study of new Schiff bases based on imidazo (1,2-a) pyridine as corrosion inhibitor of mild steel in 1M HCl", *J. Mol. Struct.*, vol. 1226, part B, pp. 129372, 2021.

[31] L. Popoola, "Organic green corrosion inhibitors (OGCIs): A critical review", *Corros. Rev.*, vol. 37, pp. 71-102, 2019.